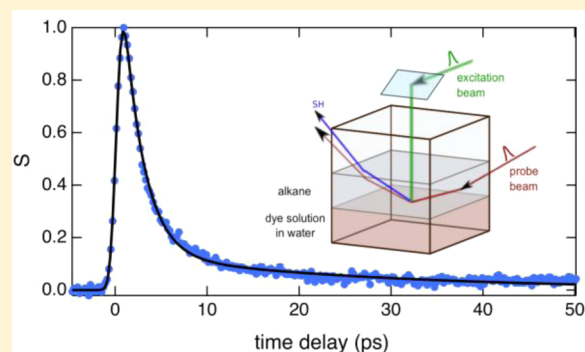


Excited-State Dynamics of Organic Dyes at Liquid/Liquid Interfaces

Marina Fedoseeva, Sabine Richert, and Eric Vauthey*

Department of Physical Chemistry, University of Geneva, 30 Quai Ernest-Ansermet, 1211 Genève 4, Switzerland

ABSTRACT: Liquid/liquid interfaces play a crucial role in numerous areas of science. However, direct spectroscopic access to this thin (~ 1 nm) region is not possible with conventional optical methods. After a brief review of the most used techniques to perform interfacial optical spectroscopy, we will focus on time-resolved surface second harmonic generation, which allows the measurement of the excited-state dynamics of probe molecules at interfaces. By comparing these dynamics with those measured in bulk solutions, precious information on the properties of the interfacial region can be obtained. To illustrate this, several studies performed in our group will be presented.



1. INTRODUCTION

The interface between two immiscible liquids has attracted the interest of scientists for a long time. This region plays an important role in many phenomena that are crucial in areas as diverse as life sciences, environmental sciences, and technology.^{1–3} Although a liquid interface can be viewed as a region segregating two bulk liquids, it does not prevent the transfer of mass and energy between them. Therefore, understanding the properties of interfaces and the dynamics of interfacial processes is of utmost importance not only for our fundamental knowledge but also for many applications such as the design of new drugs¹ or developments toward renewable energies.⁴

One peculiarity of interfaces is that the molecules located in this region experience an anisotropy of forces. As a consequence, their orientation is not random as in bulk solution, and the dynamics of molecular processes that depends on environmental properties (e.g., friction or local electric field) can be expected to be different at interfaces and in bulk solutions. In bulk materials, these properties can be directly deduced from macroscopic quantities such as the viscosity and the dielectric constant. However, the interfacial region between two immiscible liquids is very thin, typically 1 nm;⁵ therefore, the viscosity and the dielectric constant cannot be really defined. Consequently, friction and the local electric field at the interface have to be measured in situ using local probes.^{6–9} Our approach for gaining insight into interfacial properties is the so-called dynamic probe concept, where the dynamic probe is a molecule whose photophysics, for example, its excited-state lifetime, depends on a property of the environment. This approach first requires a good understanding of the excited-state dynamics of the probe in bulk solution and the dependence of these dynamics on the solvent. Once this knowledge is available, the dynamics of the probe can be investigated at interfaces and compared to that in the bulk. The way this strategy can be used to access interfacial properties will be illustrated here for friction, salt concentration, and hydrogen bonding at liquid/liquid interfaces.

Liquid interfaces offer more degrees of freedom for fine-tuning a given environmental parameter than bulk solutions because the properties of both phases can be varied independently. This can be advantageously used to obtain specific information on a probe molecule adsorbed at the interface, as will be illustrated here.

One prospect is that, once the properties of liquid interfaces are well understood, this region can be used as a specific environment for performing chemical reactions that would not be possible in bulk media such as bimolecular reactions between reactants located in different phases. Photoinduced electron transfer through liquid interfaces is one example that has a key value for a number of chemical and biological phenomena.^{4,10}

2. SPECTROSCOPIC TECHNIQUES FOR INVESTIGATING LIQUID INTERFACES

Even though interfaces are of clear fundamental scientific importance, they are a challenge to study on the molecular level. Most of the powerful and common spectroscopic techniques used for investigating molecules in bulk media cannot be readily applied to interfaces because the signal from the sample is almost entirely due to the molecules located in the bulk phases, whose number surpasses that of the interfacial molecules by many orders of magnitude. The interfacial response is thus totally buried in that from the bulk.

There are generally two conceptual approaches to studying interfaces by optical spectroscopy. In the first, the optical beams are confined close to the interface in order to reduce the relative contribution from the bulk phases to the signal. One of the experiments based on this principle was realized by Deckert and co-workers,^{11,12} who used the light from a scanning near-

Received: April 13, 2012

Revised: May 23, 2012

Published: June 8, 2012

field optical microscopy tip to perform Raman spectroscopy. By progressively moving the tip toward the interface, Raman spectra at different penetration depths relative to the interface could be measured. This technique was applied to study the water/carbon tetrachloride interface with a spatial resolution of 200 nm.¹² The OH stretching vibrational frequency of water was found to shift to higher frequencies when approaching the interface. This was interpreted in terms of weaker hydrogen bonding in the vicinity of the nonpolar phase. However, no dynamic studies have been performed with this method.

Time-resolved total internal reflection fluorescence (TR-TIRF) is another method based on the beam-confining concept. It was first demonstrated at a sapphire/polymer interface by Masuhara et al.¹³ and was later applied to liquid/liquid interfaces.^{14–16} In TR-TIRF, the probe molecules are located in the phase with the lower refractive index, whereas the phase with the higher refractive index is transparent. The probe molecules are excited by the evanescent field generated upon total internal reflection of a laser pulse striking the interface from the high-refractive-index side. Because the evanescent field has a penetration depth of typically 100 nm, fluorescence arises only from molecules located close to the interface. Using time-correlated single photon counting electronics for detection allows fluorescence dynamics measurements with a time resolution of 20–50 ps. This technique has been used successfully to investigate various excited-state processes (e.g., photoisomerization or excitation energy transfer^{15,17}) close to a liquid/liquid interface. The study of the reorientational dynamics of fluorophores near an interface is also easily accessible by measuring the decay of the fluorescence anisotropy.¹⁴

Although this method benefits from its simplicity, it is limited to the study of emissive probes. Thus, no information on the dynamics of dark species or on the mechanism of possible quenching processes can be gained from TR-TIRF measurements. Time-resolved attenuated TIR (TR-ATIR), which was demonstrated several years ago, is not impaired by this limitation.¹⁸ However, this technique suffers from poor sensitivity because of the usually very weak photoinduced changes in absorbance experienced by the evanescent field.

We tried to combine the sensitivity of fluorescence and the polyvalence of transient absorption spectroscopy by applying the transient evanescent grating technique¹⁹ first demonstrated at solid/solid and solid/liquid interfaces.^{20,21} The conventional transient grating method is based on a four-wave mixing process where two pump pulses crossed on the sample generate a spatial modulation of intensity that, upon absorption by the sample, results in spatial modulations of refractive index and absorbance (i.e., in phase and amplitude gratings²²). Probing is achieved with a third, time-delayed pulse that strikes the gratings at the Bragg angle and undergoes partial diffraction. The intensity of the diffracted pulse, I_d , the signal, is given by

$$I_d = a\Delta n^2 + b\Delta A^2 \quad (1)$$

where Δn and ΔA are the modulation amplitudes of the refractive index and absorbance, respectively, and a and b are constants. Therefore, the temporal changes in refractive index and absorbance at the probe wavelength can be monitored by measuring the signal intensity as a function of the time delay.²³ Broadband detection, allowing diffracted spectra over the whole visible range to be recorded, has also been demonstrated.²⁴ In the transient evanescent grating technique, some of the waves are evanescent fields generated upon TIR at the liquid/liquid

interface. In the simplest configuration (Figure 1A), the gratings are generated in the absorbing phase by two pump

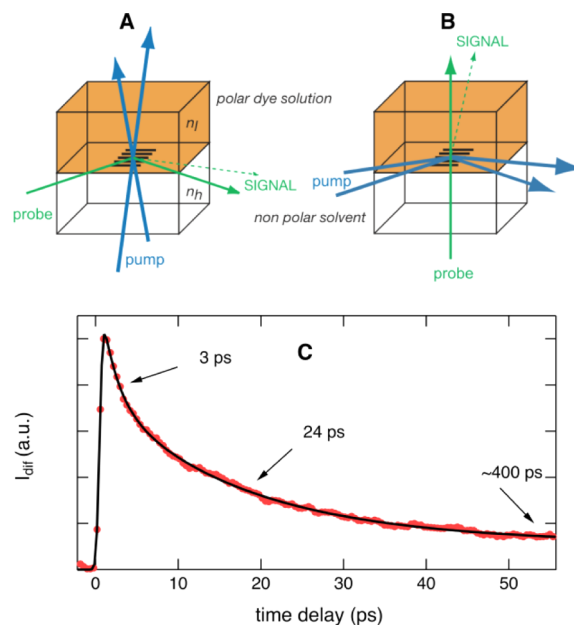


Figure 1. (A, B) Two possible beam arrangements for the transient evanescent grating technique (n_l and n_h refer to low and high refractive indices, respectively). (C) Time profile of the diffracted signal at 530 nm obtained upon excitation at the same wavelength for a solution of rhodamine 6G in methanol in contact with decalin using layout A.

pulses and interfacial selectivity is achieved by probing in TIR geometry. Only the evanescent probe field interacts with the gratings and is diffracted. In this case, the interfacial selectivity, which depends on the penetration depth of the probe field, is the same as in TR-TIRF. A better selectivity can be achieved by generating true evanescent gratings (i.e., by using two pump pulses in TIR geometry (Figure 1B)). Because the diffracted signal intensity is proportional to the square of the photoinduced changes, a gain in interfacial selectivity by a factor of 2 is realized. By measuring the time evolution of the refractive index changes, this technique has been used to investigate the thermo-acoustic properties (i.e., the speed of sound, the acoustic attenuation, and the thermal conductivity) of the region close to the interface.²⁵ However, measurements of the changes in absorbance provide access to population dynamics.¹⁹ For example, Figure 1C shows the time profile of the diffracted intensity measured at 530 nm with a 5×10^{-2} M solution of rhodamine 6G (Rh6G) in methanol close to the interface with decalin after excitation at the same wavelength. This profile reflects the recovery of the Rh6G ground-state population. Bulk measurements of the same solution show an exponential ground-state recovery (GSR) with a 500 ps time constant. This is shorter than the ~ 4 ns lifetime measured in more dilute solutions because of the occurrence of self-quenching at 5×10^{-2} M.²⁶ The multiphasic GSR measured by the transient grating was explained in terms of a gradient of Rh6G concentration probed by the evanescent field, decreasing when going from the interface toward the bulk. Therefore, the shorter decay component was assigned to the interfacial region with a high Rh6G concentration, where self-quenching is very efficient, whereas the slowest component, similar to that measured in the bulk, was ascribed to the contribution from the

deepest region probed by the evanescent field. Such multiphasic dynamics is also often encountered in TR-TIRF¹⁶ and arises from the fact that these techniques based on TIR are not intrinsically interface-selective. Indeed, the probed region is typically 50 to 100 nm thick, whereas the interfacial region has a thickness of the order of 1 nm. Although the confinement of the optical beam realized by TIR seems to be sufficient to enable the observation of molecules near an interface, it is still too large to achieve true interfacial selectivity. Therefore, discriminating the response from the molecules at the interface from that of molecules located further away can be highly problematic. Furthermore, the investigated molecules have to be in the low-refractive-index phase, limiting the choice of liquid/liquid interfaces that can be studied.

The solution to circumvent the shortcoming of this beam-confinement approach is to probe a property that is intrinsic to interfaces, namely, one that vanishes in the bulk phases. This is the case for second and higher even orders of the optical nonlinear susceptibility, $\chi^{(2n)}$.²⁷ Consequently, second-order nonlinear processes such as second-harmonic (SHG) and sum-frequency generation (SFG) are electric-dipole-forbidden in centrosymmetric media. However, the interface between two isotropic media such as two liquids is not centrosymmetric and thus possesses a nonzero $\chi^{(2n)}$. This is the principle behind the surface SHG (SSHG) technique,^{28,29} where an optical field, \vec{E} , at frequency ω_1 strikes the interface and creates a second-order nonlinear polarization oscillating at $\omega_2 = 2\omega_1$

$$\vec{P}^{(2)}(\omega_2) = \epsilon_0 \vec{\chi}^{(2)}(\omega_2, \omega_1, \omega_1) \vec{E}(\omega_1) \vec{E}(\omega_1) \quad (2)$$

where $\vec{\chi}^{(2)}$ is the second-order nonlinear optical susceptibility tensor. Neglecting local field effects, this macroscopic quantity can be related to the second-order polarizability tensor, $\vec{\beta}$, of the molecules that constitute the interface

$$\vec{\chi}^{(2)} \approx N \langle \vec{\beta} \rangle \quad (3)$$

where N is the interfacial adsorbate density (number per unit area), with the brackets indicating an average over the molecular orientations. This polarization oscillating at ω_2 is the source of a new electromagnetic field at the same frequency, the second-harmonic (SH) signal, whose intensity is

$$I_i(\omega_2) \propto |\chi_{ijk}^{(2)}(\omega_2, \omega_1, \omega_1)|^2 I_j(\omega_1) I_k(\omega_1) \quad (4)$$

where $\chi_{ijk}^{(2)}$ is a tensor element of $\vec{\chi}^{(2)}$ and subscripts i , j , and k represent the polarization direction of the three fields. The relative magnitude of these tensor elements depends on the symmetry of the material. A liquid/liquid interface has $C_{\infty v}$ symmetry that can be reduced to C_{4v} . In this case, only 7 out of the 27 elements of $\vec{\chi}^{(2)}$ are nonzero, but because some of them are identical and $x = y$, only three, namely, $xzx = xxz$, zxx , and zzz , have to be considered.³⁰

An important feature of $\chi^{(2)}$ lies in its wavelength dependence, which, for a classical anharmonic oscillator, has the following form

$$\chi^{(2)}(\omega_2, \omega_1, \omega_1) \propto \frac{1}{(\omega_{ba}^2 - \omega_2^2 - 2i\Gamma_{ba}\omega_2)(\omega_{ba}^2 - \omega_1^2 - 2i\Gamma_{ba}\omega_1)^2} \quad (5)$$

where ω_{ba} is the resonance frequency of the $|a\rangle$ to $|b\rangle$ transition and Γ_{ba} is the associated line width. Therefore, $\chi^{(2)}$ increases significantly when the incoming and/or signal fields are in

resonance with a transition of the material. Consequently, the SH intensity spectrum reflects one- and two-photon resonances of molecules located at the interfaces.²⁸ By taking advantage of the electronic resonance enhancement, the SH signal from relatively dilute ($\sim 10^{-5}$ M) probe molecules can surpass the nonresonant contribution from the solvent molecules by several orders of magnitude. The same principles underlie surface SFG (SSFG), where one of the incident fields is at fixed frequency and the other is tunable or has a broad spectrum.³¹ In most SSFG applications to liquid interfaces, the second incident field is in the IR region and the signal intensity reflects vibrational resonances.³² To be detectable, a vibrational mode has to be both IR- and Raman-active, precluding the investigation of centrosymmetric molecules, in agreement with their lack of second-order nonlinear susceptibility. It should nevertheless be noted that SSH(F)G from apparently centrosymmetric molecules cannot be excluded if these molecules are distorted at the interface.³³ As vibrational transitions generally have much smaller oscillator strengths than electronic transitions, the corresponding resonance enhancement of the signal is smaller. As a consequence, vibrational SSFG is less sensitive than electronic SSFG and SSHG and needs much more concentrated samples. For example, vibrational SSFG has been intensively used to record the vibrational spectrum of water at liquid/water and air/water interfaces.^{34–38} However, electronic SSFG has recently been demonstrated to be a very powerful method of recording the electronic spectrum of probe molecules at the air/water interface using a white light continuum as one of the incoming fields and broadband detection.^{31,39}

As a consequence of its higher sensitivity, electronic SSH(F)G can be relatively easily time-resolved.^{40–42} In this case, the probe molecules located in one of the phases are excited by a pump pulse and the variation of the SH(F) signal is recorded as a function of the time after excitation. Such probing ensures the interfacial selectivity of time-resolved (TR)-SSH(F)G.

The optical layout of the TR-SSHG setup used for the experiments described below is depicted in Figure 2. It is based on an amplified Ti:sapphire system producing ~ 100 fs pulses around 800 nm at 1 kHz. A fraction of this output is used to feed a noncollinear optical parametric amplifier (NOPA) generating ~ 50 fs pulses tunable between 480 and 700 nm.

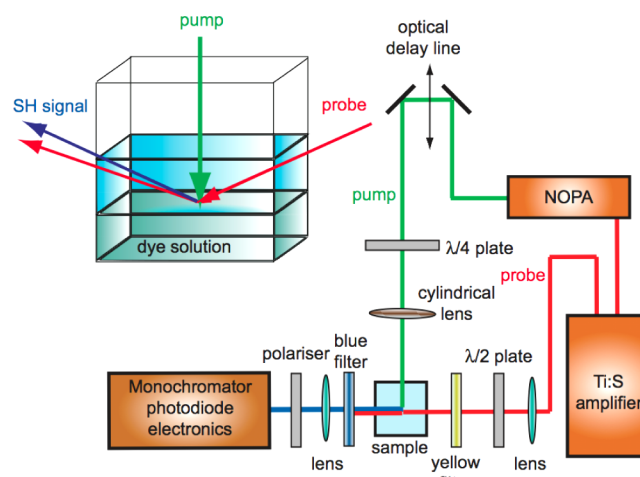


Figure 2. Schematic layout of the TR-SSHG setup.

These pulses are directed toward the interface from above through the transparent organic phase and focused with a combination of spherical and cylindrical lenses to ensure an optimal overlap with the probe pulses. The pump pulses (typically 1 to 2 μJ) excite the dye molecules dissolved in the aqueous phase with no interfacial selectivity. Circular polarization is used to prevent a photoselection of the molecules according to the orientation of their transition dipole moment in the interfacial (x - y) plane.

For SSHG probing, a small fraction of the 800 nm amplifier output (10–100 nJ) strikes the interface from the transparent and high-refractive-index phase and undergoes TIR. These probe pulses and the SH signal are reflected at the interface at different angles because of the dispersion in the transparent phase. The signal is collected with a lens, filtered out from the accompanying scattered fundamental light with a blue filter, and focused onto a monochromator equipped with a multipixel photon counter avalanche photodiode detector. The output signal is further processed with a boxcar gated integrator and averager module before being digitized and stored on a computer. The probe pulses are linearly polarized, and in order to measure specific elements of the $\chi^{(2)}$ tensor, a half-wave plate and a polarizer are located before the sample and the detector, respectively. For example, when probing with the polarization oriented 45° relative to the plane of incidence, the intensity of the s-polarized component of the SH signal is proportional to $|\chi_{xxz}^{(2)}|^2$. Unless specified, the polarization of the probe pulses was perpendicular to the plane of incidence, whereas the parallel component of the SH signal was measured. The SH intensity depends not only on the square modulus of the nonlinear susceptibility but also on geometrical factors such as the linear and nonlinear Fresnel factors for reflection. The latter have been shown to be particularly large near the critical angle for TIR.⁴³ For this reason, TIR geometry is usually used in TR-SSHG at liquid interfaces. This is, of course, not possible for air/liquid interfaces, and for this reason, the SH intensity is usually much weaker than at liquid/liquid interfaces.

Dynamic information on the photoexcited dye molecules at the interface is obtained by recording the SH intensity as a function of the temporal delay between the pump and probe pulses for given sets of polarization. In general, before doing any quantitative analysis, the data are transformed by first taking the square root of the SH intensity and subsequent normalization so that the intensity is 0 at negative time delays and 1 at its maximum. The so-processed signal intensity, S , is now proportional to the photoinduced changes of population. This procedure requires the SH signal to be purely resonant, dominated by a single resonance, and to have no nonresonant background contribution from the solvents that constitute the two phases of the interface. Figure 3 shows an example of such a profile measured with Rh6G (5×10^{-4} M) at the dodecane/water interface. In this case, the probe field is close to two-photon resonance with the $S_2 \leftarrow S_0$ transition of the dye, and the initial drop in signal intensity should mainly reflect the depletion of the ground-state population upon photoexcitation. As the excited-state population relaxes to the ground state, the signal intensity recovers its initial value. If the probe field were resonant with a transition from the excited state of the molecule, then the SSHG intensity would exhibit the opposite behavior (i.e., first an increase upon excitation and then a decay to the initial value). The decay of the excited-state population at the interface is much faster than in bulk water at similar concentrations, where it occurs on the nanosecond time scale.

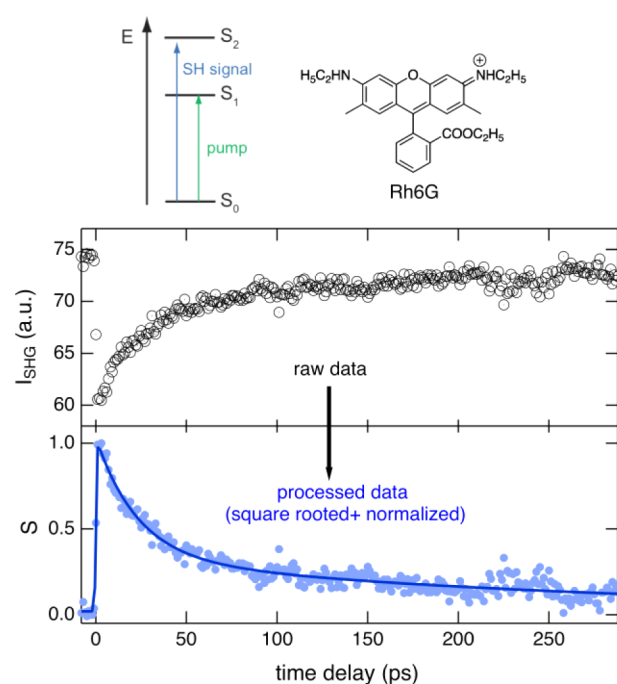


Figure 3. TR-SSHG profile recorded at 400 nm upon excitation of Rh6G at 530 nm at the dodecane/water interface. To reflect the population change better, the raw data (black circles) are processed by taking the square root and by subsequent normalization (blue circles). Because the SH signal is close to resonance with the $S_2 \leftarrow S_0$ transition and the signal decreases upon excitation, the processed profile should mostly reflect the recovery of the ground-state population.

This shortening is ascribed to the larger interfacial concentration of Rh6G and to self-quenching as already discussed above for the transient grating results. Because there is no magic angle in TR-SSHG, the reorientation of molecules at the interface could also affect the measured profiles, depending on the time scale considered.⁸

We will now illustrate how TR-SSHG, when combined with other time-resolved techniques for bulk dynamics, can deliver rich information on the dynamics of photoinduced processes at liquid interfaces.

3. PROBING INTERFACIAL FRICTION

Because of the different local properties of interfaces, solute molecules adsorbed at an interface could exhibit a reactivity that differs from that of the same molecules dissolved in the bulk. For example, the friction exerted by the environment, which in bulk solutions can be predicted from the viscosity, influences the dynamics of many chemical reactions. Because viscosity cannot be defined at a liquid interface, the friction has to be determined directly, using, for example, the dynamic probe approach. Triphenylmethane dyes such as malachite green (MG) and brilliant green (BG) are well-suited probes because the lifetime of their lowest singlet excited state depends on the viscosity. MG has been the subject of numerous time-resolved spectroscopic experiments to understand the origin of the ultrafast nonradiative relaxation of its S_1 state in solution.^{44,45} Moreover, MG has already been shown to be a very good interfacial probe for TR-SSHG studies.^{46,47} It is generally agreed that the process is intrinsically barrierless and involves the motion of the aniline and/or phenyl substituents around the single bond to the central carbon atom. The friction exerted by the environment on the rotating rings leads to the viscosity

dependence of the excited-state lifetime. However, a few questions regarding the deactivation pathway of MG remained unanswered. For example, the nature of the state populated directly upon internal conversion from the S_1 state has been questioned. To clarify this issue and to calibrate the viscosity dependence of the S_1 lifetime of MG and BG precisely, their excited-state dynamics was investigated by transient absorption spectroscopy in water–glycerol solutions of various compositions.⁴⁸ The dynamics could be well reproduced by assuming an $A \rightarrow B \rightarrow C \rightarrow D$ scheme, where the $A \rightarrow B$ step occurs on the subpicosecond time scale, independently of viscosity, and the time constants of the $B \rightarrow C$ and $C \rightarrow D$ steps exhibit a $\tau \propto \eta^\alpha$ viscosity dependence with $\alpha \approx 0.6$ and 0.75 for MG and BG, respectively. From this analysis, the intermediates could be identified with the Franck–Condon (A) and the vibrationally relaxed S_1 states (B) and the twisted (C) and the relaxed S_0 states (D).

After MG was properly calibrated as a dynamic probe for friction, its excited-state dynamics was measured at the air/water interface by TR-SSHG.⁴⁹ For these measurements, MG was excited to the S_1 state at 615 nm and probing was done at 800 nm, with the SH signal at 400 nm being in resonance with the $S_2 \leftarrow S_0$ transition. The resulting time profile was qualitatively similar to that shown in Figure 3, and the processed intensity, $S(t)$, could be well reproduced using a biexponential function with 1–2 and ~ 10 –20 ps time constants, in good agreement with measurements by other groups.^{46,47} Whereas the shorter time constant could be ascribed to the decay of the excited state (i.e., to the $B \rightarrow C$ step), the assignment of the 20 ps component was more ambiguous and will be discussed in more detail below. The 1–2 ps S_1 lifetime of MG at the air/water interface should be compared to the 570 fs found in bulk water. The friction exerted by interfacial water is clearly larger than that exerted by bulk water, pointing to an arrangement of water molecules at the interface that results in a more rigid structure. According to polarization-dependent SSHG measurements, the polar aniline groups of MG are located in the aqueous phase whereas the phenyl group points toward the nonpolar phase.⁴⁶ The motion of the aniline groups is thus unambiguously involved in the nonradiative relaxation of the S_1 state of MG. To find out whether the S_1 -state lifetime of MG also follows an η^α dependence at the interface and to be able to vary the viscosity of both phases, the measurements were performed at liquid/liquid interfaces.⁴⁸ First, the bulk viscosity of the nonpolar phase was kept constant, whereas that of the aqueous phase was changed by adding various amounts of glycerol. The interfacial GSR dynamics of MG and BG was found to follow an η^α dependence as well (Figure 4B). However, α was around 0.4 for both MG and BG, substantially smaller than the bulk values of 0.6 and 0.75. This implies that although the excited-state lifetime is always longer at the interface than in the bulk, this difference decreases with increasing glycerol concentration. There might be several reasons for this effect. The most evident one is that the addition of glycerol affects interfacial friction less than bulk friction. This could be due to different compositions of the water–glycerol mixtures or to different hydrogen bond networks. However, other factors such as an orientation of the dyes depending on the glycerol fraction cannot be excluded.

Another question concerning the excited-state dynamics of MG and BG was whether a large-amplitude motion of the phenyl group is also involved in the nonradiative deactivation of the S_1 state. Previous TR-SSHG measurements of MG at

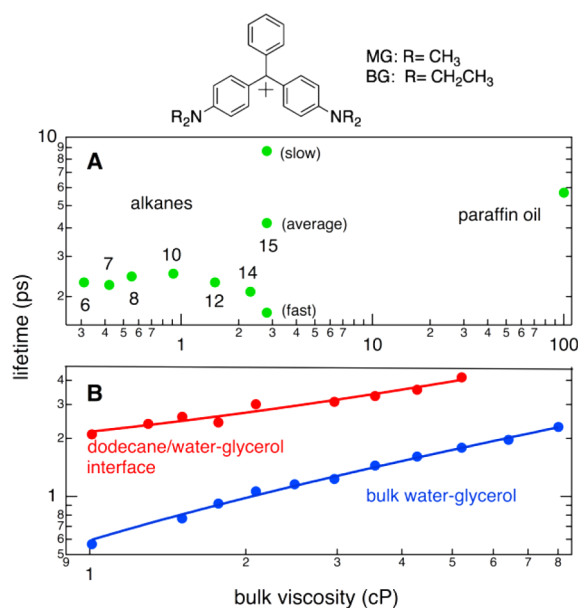


Figure 4. Viscosity dependence of the excited-state lifetime of MG at alkane/water–glycerol interfaces. Variation of the viscosity of (A) the alkane phase (the numbers indicate the number of carbon atoms of the alkane; the decay in pentadecane is biphasic and both time constants and the average are given) and (B) the aqueous phase and a comparison with the lifetime in bulk solutions.

octane/water and pentane/water interfaces pointed to the same excited-state decay time, indicating a negligible role of the phenyl group.⁴⁶ Measurements from our group confirmed this result with seven alkanes up to tetradecane with an S_1 lifetime of around 2 ps.⁴⁸ However, a 5.7 ps lifetime was measured when going to the much more viscous paraffin, showing that the hindrance of the phenyl group twist also slows down the excited-state decay of MG (Figure 4A). Higher friction is required to slow down the reorientation of the smaller, nonpolar phenyl group relative to the larger, polar aniline groups. It is probable that the interfacial friction of alkane with a bulk viscosity of <2.1 cP is too weak to slow down the motion of the phenyl group below that of the anilines in water.

This investigation shows that TR-SSHG measurements can yield information not only on the interfacial properties (friction in this case) but also on the probe itself (i.e., the involvement of the phenyl group). This latter idea has been further exploited to gain new insight into the mechanism of the nonradiative deactivation of hemicyanines (Figure 5)⁵⁰ whose fluorescence quantum yield and lifetime have been shown to increase substantially with the viscosity of the environment because of the efficient nonradiative deactivation channel of the S_1 state involving intramolecular coordinates with large-amplitude motion.⁵¹ The studied hemicyanines differed by the length of the alkyl chain (C_2H_9 or $C_{15}H_{33}$) on the dialkylamino group. In principle, torsion around four different bonds, ϕ_1 – ϕ_4 , could be responsible for the nonradiative deactivation, and several studies have been devoted to the identification of the relevant one.^{51,52} It was concluded that the trans–cis isomerization around the central bond, ϕ_3 , is not involved because of a negligible photoisomerization yield and that the twist of the dialkylamino group, ϕ_1 , is associated with too high a barrier.⁵² Thus, the two remaining coordinates are the twists of the dialkylaniline, ϕ_2 , and the pyridinium group, ϕ_4 . One way to determine the relevant coordinate could be comparing the

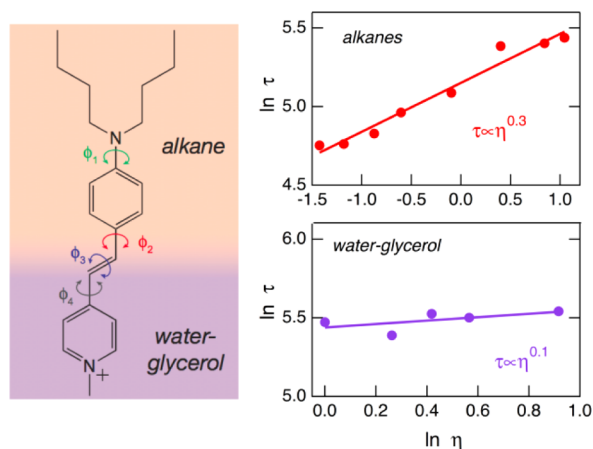


Figure 5. Viscosity dependence of the excited-state lifetime of a hemicyanine at alkane/water–glycerol interfaces measured by TR-SSHG.

excited-state dynamics of analogues with bond torsion blocked upon substitution with bulky groups or upon selective bridging. However, this strategy is not only costly in terms of synthetic effort but may also lead to erroneous conclusions if the electronic structure of the molecule is changed. Both hemicyanines are amphiphilic, and their orientation at the liquid/liquid interface is almost perpendicular to the charged pyridinium head in the polar phase and the dialkylaniline end in the nonpolar phase. Therefore, the possible occurrence of large-amplitude motion in these two different parts of the molecules can be investigated by measuring their excited-state lifetime by TR-SSHG while independently varying the viscosity of the polar and nonpolar phases.⁵⁰ TR-SSHG measurements were first performed upon $S_1 \leftarrow S_0$ excitation of the hemicyanines at alkane/water interfaces while keeping the viscosity of the aqueous phase constant and varying that of the nonpolar phase from 0.3 to 3 cP by going from pentane to pentadecane. The TR-SSHG profiles were dominated by a component increasing from 120 to 330 ps in this viscosity range. Because probing was done in two-photon resonance with the $S_1 \leftarrow S_0$ transition, the TR-SSHG profiles reflect mainly the GSR dynamics of the hemicyanines. These time constants followed an η^α dependence, with α amounting to 0.3 and 0.5 for the hemicyanine with short and long alkyl chains, respectively. In a second series of measurements, the upper nonpolar phase was kept unchanged whereas the viscosity of the polar phase was varied from 1 to 4 cP using water–glycerol mixtures of different compositions. An analysis of the viscosity dependence of the TR-SSHG profiles gave α values of around 0.1 for both molecules (Figure 5).

These interfacial measurements revealed that the non-radiative decay of the S_1 state of these molecules is due to large-amplitude motion of the part of the molecules located in the nonpolar phase. Considering the amphiphilic nature of these molecules, it is reasonable to assume that only the N,N -dialkylaniline tail is in the nonpolar phase. Consequently, our observation of a viscosity dependence arising exclusively from the nonpolar phase points to the rotation of this group (i.e., ϕ_2) as the mode associated with the nonradiative deactivation of these molecules. Even if it occurs, the large-amplitude motion of the pyridinium group around ϕ_4 should not play any significant role in this deactivation.

4. EFFECT OF SALTS ON AGGREGATION AT LIQUID INTERFACES

When studying the concentration dependence of the TR-SSHG profiles of MG at alkane/water interfaces, it was found that the dynamics was only biphasic above $\sim 5 \times 10^{-6}$ M and that the relative amplitude of the slow component increased up to about 0.2 at 5×10^{-5} M and then remained mostly constant.⁴⁸ This slow component was ascribed to interfacial MG aggregates, for which large-amplitude motion is hindered and nonradiative transition to the ground state is slower. The aggregation of MG in bulk solution occurs only at very high concentrations. However, aggregation in a 10^{-5} M aqueous solution of MG can be provoked by the addition of a salt such as NaCl.

The effect of ions on the property of water and the solubility of molecules, including proteins, in aqueous solutions has been a subject of intense research and discussion for many decades.^{53,54} Ions are generally sorted into series, so-called Hofmeister or lyotropic series, according to their salting-in or salting-out properties.⁵⁵ For example, the thiocyanate anion, SCN^- , favors the solubility of proteins and is thus considered to be a good salting-in ion. These Hofmeister series are also correlated with other properties of solutions such as surface tension and protein stability.^{53,55} Whereas these series of cations and anions are well established for bulk solutions, our knowledge about the effect of ions on aqueous interfaces is poorer.^{56,57} One could intuitively think that the concentration of ions at an aqueous interface is much smaller than in the bulk because of the reduced solvation. If this were the case, the addition of salt to an aqueous solution should have little direct effect on the interfacial properties. However, indirect effects could be expected for the increased adsorption of a solute at the interface upon addition of a salting-out ion. To test this, we have investigated the effect of salt on the excited-state dynamics of MG oxalate at liquid interfaces.⁵⁸ The addition of sodium salts was found to lead to two effects: (1) an increase in the stationary SSHG intensity and (2) an increase in the amplitude of the slow TR-SSHG component (Figure 6).^{49,58} Both effects were attributed to the augmentation of MG concentration and aggregation at the interface. The magnitudes of these effects were found to depend strongly on the nature of the anion. Indeed, the increase in aggregation upon addition of salt is much larger and faster with SCN^- than with Cl^- (Figure 6B,C). This seems to disagree with predictions based on the Hofmeister series, according to which SCN^- is a much better salting-in agent than Cl^- . Therefore, a decrease in the interfacial concentration of MG and thus of the aggregation would have been expected with SCN^- , contrary to observation.

However, this result can be explained if we consider that SCN^- has a stronger affinity for the interface than does Cl^- .^{59,60} In this case, the addition of NaSCN leads to an accumulation of SCN^- at the interface and to a globally negatively charged interface (Figure 7). Because MG is a cation, electrostatic interactions favor the adsorption of MG at the interface and thus its aggregation. This affinity of SCN^- for oil/water interfaces is in full agreement with its ability to denature proteins. As a consequence, the amplitude of the aggregation enhancement measured by TR-SSHG upon addition of salt reflects the anion population at the interface relative to the bulk. Aggregation does not increase much with NaCl, indicating that the interfacial concentration of Cl^- is not much larger than the bulk concentration. Therefore, it appears that the affinity of the anion for the interface correlates with the Hofmeister series

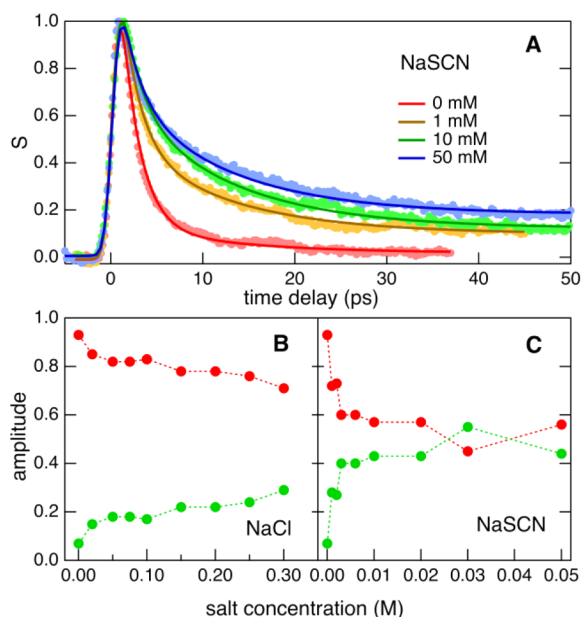


Figure 6. (A) TR-SSHG profiles recorded with MG at the dodecane/water interface with various concentrations of NaSCN and best fits from the global biexponential analysis with $\tau_1 = 2.1$ ps and $\tau_2 = 13$ ps. (B,C) Salt concentration dependence of the relative amplitudes of the fast (red) and slow (green) components of the TR-SSHG decay.

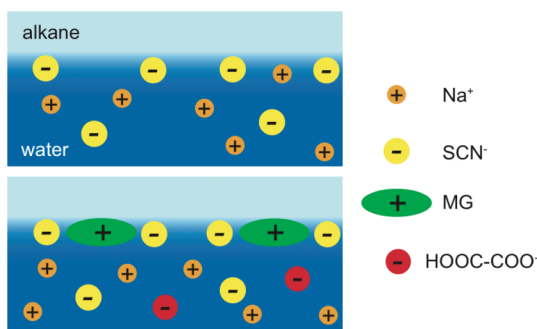


Figure 7. Schematic representation of the affinity of thiocyanate for the interface (top) and of its effect on the adsorption of MG at the interface (bottom).

as well. This can be understood by considering that the anions at the salting-in end of the series are relatively large and singly charged and thus tend to accumulate at the interface, whereas those at the other end are small and/or doubly charged and are strongly stabilized by solvation.

The observed increase in aggregation could be quantitatively well accounted for using a modified Frumkin–Fowler–Guggenheim model,⁵⁷ where the adsorption of salt anions at the interface leads to a shift of the equilibrium constant between interfacial and bulk MG in favor of the former.

There is also a Hofmeister series for cations, even though the differences are not as marked as for the anions.^{55,61} One particularly interesting cation is guanidium (GuH^+), which is also a strong protein denaturant. According to recent molecular dynamics simulations,⁶² the population of GuH^+ cations oriented parallel to the interface is larger at the interface than in the bulk, although the overall interfacial concentration is smaller. The addition of GuHCl was found to have no effect on the TR-SSHG profiles of MG at alkane/water interfaces, indicating that the aggregation of MG is not enhanced. This

suggests that the interface is overall neutral and that GuH^+ and Cl^- have similar affinities for the interface. TR-SSHG measurements using an anionic dye probe instead of cationic MG are in process to investigate the Hofmeister series of cations further.

Although this approach, based on the aggregation of a charged dye probe, is not as direct as the detection of ions by vibrational SSFG or electronic SSHG,^{57,60,63,64} it allows the investigation of a large number of different salts with a single probe molecule.

5. INTERMOLECULAR HYDROGEN BONDING AT LIQUID INTERFACES

When searching for dye probes to investigate the Hofmeister series of cations, we found eosin B (EB) to be an interesting candidate because it is doubly anionic and it has already been investigated by SSHG.⁶⁵ However, when looking for photo-physical data in the literature, we were confronted with somehow contradictory information. For instance, the fluorescence lifetimes of EB in alcohols ranging from 90 ps in methanol to 4.5 and 5.3 ns in ethanol can be found. However, the fluorescence lifetime of the closely related eosin Y (EY), where bromine atoms replace the nitro groups of EB, varies from 1.1 ns in water to 3–4.5 ns in organic solvents. Therefore, before performing TR-SSHG experiments with EB, we first reinvestigated its excited-state properties in bulk solutions using transient absorption and time-resolved fluorescence (Figure 8).⁶⁶ Rather surprisingly, we found that the excited-state

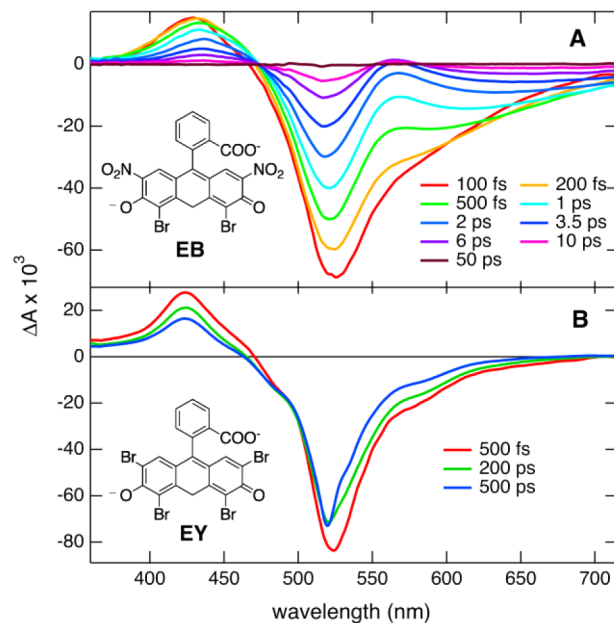


Figure 8. Transient absorption spectra recorded with (A) EB and (B) EY in water at several time delays after 520 nm excitation. The positive band is due to S_1 state absorption whereas the negative band is due to both the bleach of the ground-state absorption and the stimulated emission.

dynamics of EB, contrary to that of EY, exhibits a strong solvent dependence. Indeed, whereas for EB the S_1 -state lifetime varies from 4.3 ps in water to about 300 ps in decanol, for EY it is larger than 1 ns in all solvents investigated. In the case of EB, a good correlation between the fluorescence lifetime and the Kamlet–Taft parameter that accounts for the H-bond-donating

ability of the solvent can be found, pointing to the H-bond-assisted deactivation of the S_1 state. The fact that this effect is observed with EB and not with EY can be understood by considering that the $S_1 \leftarrow S_0$ excitation of EB is associated with substantial charge transfer toward the nitro groups and thus with an increased H-bonding interaction with the solvent at the nitro groups. This situation is known to favor H-bond-assisted nonradiative deactivation, whose exact mechanism still needs to be fully established.^{67,68} In conclusion, the nanosecond lifetime reported for EB in ethanol is probably due to confusion with EY. More interestingly, this study revealed that EB is an excellent dynamic probe for H bonding to the solvent, and the measurement of its excited-state lifetime by TR-SSHG could give valuable information about intermolecular H bonding at liquid/water interfaces. Because aggregation is a rather universal property of organic dyes at liquid/water interfaces, the effect of bulk EB concentration on the TR-SSHG profile recorded at 400 nm upon excitation at 515 nm was first investigated.⁶⁹ A substantial acceleration of the GSR dynamics of EB with increasing bulk concentration was observed at the dodecane/water interface. Additionally, the dependence of the SH intensity on the polarization was also found to depend on concentration. These effects pointed to interfacial aggregation, with xanthene dye aggregates being known to have a much shorter excited-state lifetime than the monomers because of very efficient nonradiative deactivation.⁷⁰ Interestingly, the same measurements at the decanol/water interface did not reveal any concentration dependence, indicating a marked influence of the nature of the organic phase on the properties of interfacial water.

Figure 9 depicts a comparison of TR-SSHG profiles at 400 nm measured at dodecane/water and decanol/water interfaces with transient absorption profiles recorded in bulk water and decanol at a wavelength reflecting the GSR of EB.⁶⁹ It is clear that, even with the significant contribution of aggregates at higher EB concentrations, the decays measured at the

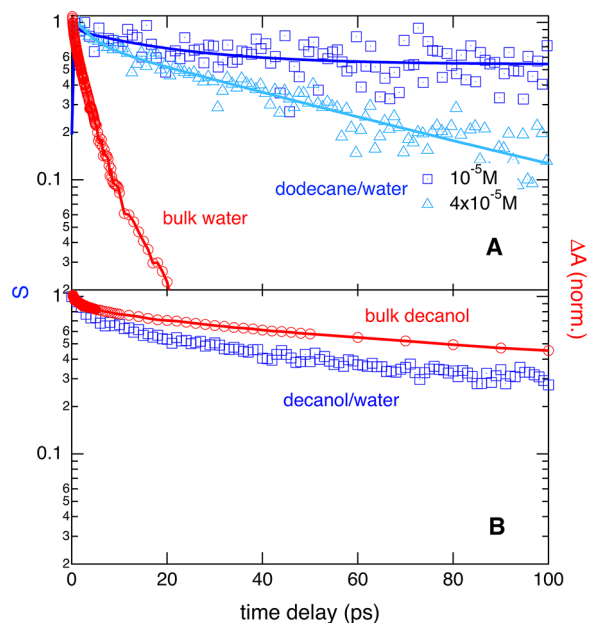


Figure 9. Comparison of the ground-state recovery dynamics of EB measured in bulk solutions by transient absorption (red) and at interfaces by TR-SSHG (blue) for (A) water and dodecane/water at two EB concentrations and (B) decanol and decanol–water.

dodecane/water interface are all much slower than in bulk water. At the lowest EB concentration investigated, the TR-SSHG signal at the dodecane/water interface is dominated by a slow, >1 ns decay component, whereas the S_1 lifetime of EB in bulk water is on the order of a few picoseconds. This huge difference indicates that most EB molecules at the dodecane/water interface are not H bonded to water molecules or at least do not undergo H-bond-assisted nonradiative deactivation. The excited-state lifetime of EB at the decanol/water interface is also much slower than in bulk water but is faster than in bulk decanol. This clearly points to the different nature of the decanol/water interface, where H bonding between the hydroxyl groups of decanol and water can be expected. Most probably, the very dissimilar H-bond motifs at these two interfaces are responsible for the different excited-state properties of EB. Clearly, further investigation is needed before a comprehensive picture of these two interfaces can be obtained.

The above findings may also be summarized in a different way: the S_1 state of EB that is nonfluorescent in aqueous solutions becomes long-lived and thus fluorescent once EB is adsorbed at a liquid/water interface. This opens the possibility to study interfaces by fluorescence techniques if the ratio of adsorbed to bulk EB molecules is sufficiently large to make the bulk background fluorescence negligible.

6. TOWARD PHOTOINDUCED ELECTRON TRANSFER AT LIQUID INTERFACES

All of the above-mentioned investigations concern intramolecular processes that cannot really be considered to be chemical reactions. Electron transfer (ET) can be regarded as the simplest chemical reaction, where the smallest chemically relevant particle is displaced from one molecule, the donor, to another, the acceptor.⁷¹ There are several reasons for investigating ET at liquid/liquid interfaces. For example, a dynamic probe could be based on photoinduced ET because the rate constant of an ET process depends strongly on environmental parameters such as the polarity, dielectric relaxation, and viscosity.⁷² For more practical applications, bimolecular photoinduced ET at liquid interfaces between two reactants confined in different phases offers an interesting perspective for efficient charge separation, which is a crucial factor in solar energy conversion.⁴ Eisenthal and co-workers have already demonstrated TR-SSHG measurements of photoinduced ET at a liquid interface.⁷³ In this case, ET took place from an aniline derivative that constituted the organic phase to excited coumarin located in the aqueous phase. We are also investigating bimolecular photoinduced ET, but in our case, the donor is not a pure solvent but is dissolved in one of the phases. One system currently under study is the EB/1,4-diazabicyclo(2.2.2)octane (DABCO) pair, where DABCO acts as an electron donor. Transient absorption measurements in acetonitrile revealed that the ET quenching of EB in the S_1 state by DABCO is diffusion-controlled and that the charge recombination (CR) of the ensuing radical pair is even faster. Such measurements were not performed in bulk water because of the very short S_1 lifetime of EB because of H-bond-assisted nonradiative deactivation.

Figure 10B shows TR-SSHG profiles recorded upon the excitation of EB with different concentrations of DABCO at the dodecane/water interface. In this case, both reactants are in the aqueous phase. The fast recovery dynamics of the signal without DABCO is due to the presence of aggregates at the

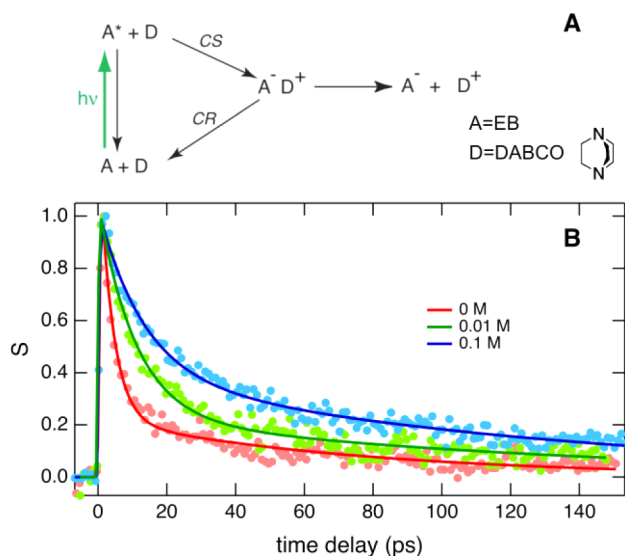


Figure 10. (A) Simplified scheme of a photoinduced electron-transfer reaction and (B) TR-SSHG profiles at 400 nm measured upon excitation of EB at the dodecane/water interface at 515 nm with different concentrations of DABCO.

relatively high EB concentration (10^{-4} M) used to ensure a sufficient signal-to-noise ratio. Interestingly, this recovery slows down with increasing DABCO concentration. At the moment, no definitive explanation can be singled out to account for this slowing down of the GSR dynamics of EB in the presence of DABCO. However, if ET between EB and DABCO occurs at the interface, as expected from bulk measurements, a second pathway for the recovery of the EB ground state is open (Figure 10A). This additional channel depends on the dynamics of both the ET quenching itself and the CR of the resulting radical pair. These are two consecutive processes, and the slowest determines the GSR dynamics. In the present case, the rate-determining process cannot be the ET quenching because its dynamics becomes faster with increasing quencher concentration. Consequently, the rate-determining step should be the recombination of the radical pair. The contribution of this slower GSR pathway depends only on the quenching efficiency of EB and should thus increase upon addition of DABCO, as observed here. However, a decrease in the aggregation upon addition of DABCO as the origin of the slowing down of the GSR cannot be totally excluded, and additional measurements are still required to substantiate the ET hypothesis.

7. CONCLUDING REMARKS AND OUTLOOK

We hope that, with this nonexhaustive overview, we could convince the reader that liquid/liquid interfaces represent a challenging and exciting playground for both spectroscopists and photochemists. At the moment, our knowledge concerning the dynamics of photoinduced processes at these interfaces is still poor, and efforts in several directions are required. For example, the current choice of molecules for sensing specific properties of liquid interfaces is not sufficient, and clearly more interfacial probes are needed. Although very powerful, TR-SSHG spectroscopy in its present state suffers from several limitations. Some of them, such as the uncertainty concerning the thickness of the interfacial region that contributes to the signal, cannot be readily eliminated. However, there is much room for improvement. For example, TR-SSHG is mostly performed at a single probe wavelength, making an

unambiguous interpretation of the resulting time profile often problematic. Clearly, probing at many different wavelengths would greatly facilitate the interpretation and allow more complicated processes to be investigated. With the availability of parametric amplifiers allowing easy tuning of the probe wavelength, this is within reach. Broadband probing and detection as recently demonstrated for electronic TR-SSFG at the air/water interface should also be considered.³⁹ Access to transient SH spectra similar to those obtained in transient absorption spectroscopy would give a strong boost to our understanding of interfacial dynamics. However, such experimental advances would be fully exploitable only if theoretical methods able to calculate the shape and intensity of transient SH spectra are available.⁷⁴ This is obviously quite a challenge, but recent results on the calculation of electronic spectra at vapor/liquid interfaces show that this is not an unrealistic task.⁷⁵

However, we should not be discouraged by these difficult tasks but should rather be stimulated by the foreseen rewards (i.e., an increased understanding of the properties of this infinitesimal but pivotal region).

AUTHOR INFORMATION

Corresponding Author

*E-mail: eric.vauthey@unige.ch.

Notes

The authors declare no competing financial interest.

ACKNOWLEDGMENTS

We thank all the previous group members who have been associated with our studies on liquid interfaces. This work was supported by the Fonds National Suisse de la Recherche Scientifique through project no. 200020-124393, the NCCR MUST, and the University of Geneva.

REFERENCES

- (1) Volkov, A. G. E. *Liquid Interfaces in Chemical, Biological, and Pharmaceutical Applications*; Marcel Dekker: New York, 2001.
- (2) Watarai, H.; Teramae, N.; Sawada, T. *Interfacial Nanochemistry*; Kluwer Academic: New York, 2005.
- (3) Adamson, A. W. *Physical Chemistry of Surfaces*, 4th ed.; Wiley: New York, 1982.
- (4) Fermin, D. J.; Duong, H. D.; Ding, Z.; Brevet, P. F.; Girault, H. H. Solar energy conversion using dye-sensitized liquid/liquid interfaces. *Electrochem. Commun.* **1999**, *1*, 29.
- (5) Steel, W. H.; Walker, R. A. Measuring dipolar width across liquid-liquid interfaces with 'molecular rulers'. *Nature* **2003**, *424*, 296.
- (6) Tamburello Luca, A. A.; Hebert, P.; Brevet, P. F.; Girault, H. H. Surface second-harmonic generation at air/solvent and solvent/solvent interfaces. *J. Chem. Soc., Faraday Trans.* **1995**, *91*, 1763.
- (7) Walker, D. S.; Richmond, G. L. Interfacial depth profiling of the orientation and bonding of water molecules across liquid-liquid interfaces. *J. Phys. Chem. C* **2008**, *112*, 201.
- (8) Shang, X.; Nguyen, K.; Rao, Y.; Eiselthal, K. B. In-plane molecular rotational dynamics at a negatively charged surfactant/aqueous interface. *J. Phys. Chem. C* **2008**, *112*, 20375.
- (9) Nihonyanagi, S.; Ishiyama, T.; Lee, T.-k.; Yamaguchi, S.; Bonn, M.; Morita, A.; Tahara, T. Unified molecular view of the air/water interface based on experimental and theoretical $\chi^{(2)}$ spectra of an isotopically diluted water surface. *J. Am. Chem. Soc.* **2011**, *133*, 16875.
- (10) Jin, Q.; Bethke, C. M. Kinetics of electron transfer through the respiratory chain. *Biophys. J.* **2002**, *83*, 1797.
- (11) De Serio, M.; Bader, A. N.; Heule, M.; Zenobi, R.; Deckert, V. A near-field optical method for probing liquid-liquid interfaces. *Chem. Phys. Lett.* **2003**, *380*, 47.

- (12) De Serio, M.; Mohapatra, H.; Zenobi, R.; Deckert, V. Investigation of the liquid-liquid interface with high spatial resolution using near-field Raman spectroscopy. *Chem. Phys. Lett.* **2006**, *417*, 452.
- (13) Masuhara, H.; Mataga, N.; Tazuke, S.; Muraio, T.; Yamazaki, I. Time-resolved total internal reflection fluorescence spectroscopy of polymer films. *Chem. Phys. Lett.* **1983**, *100*, 415.
- (14) Sassaman, J. L.; Wirth, M. J. Reorientation of acridine orange at an alcohol-modified liquid/liquid interface. *Colloids Surf., A* **1994**, *93*, 49.
- (15) Ishizaka, S.; Habuchi, S.; Kim, H.-B.; Kitamura, N. Excitation energy transfer from sulforhodamine 101 to acid blue 1 at a liquid/liquid interface: experimental approach to estimate interfacial roughness. *Anal. Chem.* **1999**, *71*, 3382.
- (16) Pant, D.; Girault, H. H. Time-resolved total internal reflection fluorescence spectroscopy. Part I. Photophysics of coumarin 343 at liquid/liquid interface. *Phys. Chem. Chem. Phys.* **2005**, *7*, 3457.
- (17) Yao, H.; Kitagawa, F.; Kitamura, N. Photoisomerization of DODCI at a solid/liquid interfaces studied by steady state and time-resolved total internal reflection fluorescence spectroscopy. *Langmuir* **2000**, *16*, 3454.
- (18) Tsukahara, S.; Watarai, H. Transient attenuated total internal reflection spectroscopy to measure the relaxation kinetics of triplet state of tetra(N-methylpyridinium-4-yl)porphine at liquid-liquid interface. *Chem. Lett.* **1999**, *28*, 89.
- (19) Brodard, P.; Vauthey, E. Exploring liquid/liquid interfaces with transient evanescent grating techniques. *Rev. Sci. Instrum.* **2003**, *74*, 725.
- (20) Tamai, N.; Asahi, T.; Ito, T. In *Microchemistry, Spectroscopy and Chemistry in Small Domains*; Masuhara, H., DeSchryver, F. C., Kitamura, N., Tamai, N., Eds.; Elsevier Science: Amsterdam, 1994; p 241.
- (21) Terazima, M.; Kojima, Y.; Hirota, N. Dynamics of a liquid crystal molecule at a solid-liquid interface detected by the time-resolved transient grating method. *Chem. Phys. Lett.* **1996**, *259*, 451.
- (22) Fourkas, J. T.; Fayer, M. D. The transient grating: a holographic window to dynamic processes. *Acc. Chem. Res.* **1992**, *25*, 227.
- (23) Gummy, J.-C.; Vauthey, E. Picosecond polarization grating study of the effect of excess excitation energy on the rotational dynamics of rhodamine 6G in different electronic states. *J. Phys. Chem.* **1996**, *100*, 8628.
- (24) Högemann, C.; Pauchard, M.; Vauthey, E. Picosecond transient grating spectroscopy: the nature of the diffracted spectrum. *Rev. Sci. Instrum.* **1996**, *67*, 3449.
- (25) Brodard, P.; Vauthey, E. Application of transient evanescent grating technique to the study of liquid/liquid interfaces. *J. Phys. Chem. B* **2005**, *109*, 4668.
- (26) Penzkofer, A.; Lu, Y. Fluorescence quenching of rhodamine 6G in methanol at high concentration. *Chem. Phys.* **1986**, *103*, 399.
- (27) Boyd, R. W. *Nonlinear Optics*; Academic Press: Boston, 1992.
- (28) Heinz, T. F.; Chen, C. K.; Ricard, D.; Shen, Y. R. Spectroscopy of molecular monolayers by resonant second-harmonic generation. *Phys. Rev. Lett.* **1982**, *48*, 478.
- (29) Brevet, P.-F. *Surface Second Harmonic Generation*; Presses Polytechniques et Universitaires Romandes: Lausanne, Switzerland, 1997.
- (30) Eienthal, K. B. Liquid interfaces probed by second-harmonic and sum-frequency spectroscopy. *Chem. Rev.* **1996**, *96*, 1343.
- (31) Yamaguchi, S.; Tahara, T. Precise electronic $\chi^{(2)}$ spectra of molecules adsorbed at an interface measured by multiplex sum frequency generation. *J. Phys. Chem. B* **2004**, *108*, 19079.
- (32) Richmond, G. L. Molecular bonding and interactions at aqueous surfaces as probed by vibrational sum frequency spectroscopy. *Chem. Rev.* **2002**, *102*, 2693.
- (33) Echevarria, L.; Nieto, P.; Gutiérrez, H.; Mújica, V.; Caetano, M. SHG of ultrathin films of metal porphyrins on BK7 glass in total internal reflection geometry: theory and experiments. *J. Phys. Chem. B* **2003**, *107*, 9332.
- (34) Scatena, L. F.; Brown, M. G.; Richmond, G. L. Water at Hydrophobic surfaces: weak hydrogen bonding and strong orientation effects. *Science* **2001**, *292*, 908.
- (35) Moore, F. G.; Richmond, G. L. Integration or segregation: how do molecules behave at oil/water interfaces? *Acc. Chem. Res.* **2008**, *41*, 739.
- (36) Chen, X.; Hua, W.; Huang, Z.; Allen, H. C. Interfacial water structure associated with phospholipid membranes studied by phase-sensitive vibrational sum frequency generation spectroscopy. *J. Am. Chem. Soc.* **2010**, *132*, 11336.
- (37) Nihonyanagi, S.; Yamaguchi, S.; Tahara, T. Water hydrogen bond structure near highly charged interfaces is not like ice. *J. Am. Chem. Soc.* **2010**, *132*, 6867.
- (38) Eftekhari-Bafrooei, A.; Borguet, E. Effect of hydrogen-bond strength on the vibrational relaxation of interfacial water. *J. Am. Chem. Soc.* **2010**, *132*, 3756.
- (39) Sekiguchi, K.; Yamaguchi, S.; Tahara, T. Femtosecond time-resolved electronic sum-frequency generation spectroscopy: a new method to investigate ultrafast dynamics at liquid interfaces. *J. Chem. Phys.* **2008**, *128*, 114715.
- (40) Shank, C. V.; Yen, R.; Hirlimann, C. Femtosecond-time-resolved surface structural dynamics of optically excited silicon. *Phys. Rev. Lett.* **1983**, *51*, 900.
- (41) Shannon, V. L.; Koos, D. A.; Robinson, J. M.; Richmond, G. L. Optical second-harmonic generation as an in-situ probe of electrode surface dynamics. Ag(111). *Chem. Phys. Lett.* **1987**, *142*, 323.
- (42) Sitzmann, E. V.; Eienthal, K. B. Picosecond dynamics of a chemical reaction at the air-water interface studied by surface second harmonic generation. *J. Phys. Chem.* **1988**, *92*, 4579.
- (43) Bloembergen, N.; Simon, H. J.; Lee, C. H. Total reflection phenomena in second harmonic generation of light. *Phys. Rev.* **1969**, *181*, 1261.
- (44) Ippen, E. P.; Shank, C. V.; Bergman, A. Picosecond recovery dynamics of malachite green. *Chem. Phys. Lett.* **1976**, *38*, 611.
- (45) Nagasawa, Y.; Ando, Y.; Kataoka, D.; Matsuda, H.; Miyasaka, H.; Okada, T. Ultrafast excited state deactivation of triphenylmethane dyes. *J. Phys. Chem. A* **2002**, *106*, 2024.
- (46) Shi, X.; Borguet, E.; Tarnovsky, A. N.; Eienthal, K. B. Ultrafast dynamics and structure at aqueous interfaces by second harmonic generation. *Chem. Phys.* **1996**, *205*, 167.
- (47) Sen, P.; Yamaguchi, S.; Tahara, T. Ultrafast dynamics of malachite green at the air-water interface studied by femtosecond time-resolved electronic sum frequency generation (TR-ESFG): an indicator for local viscosity. *Faraday Discuss* **2010**, *145*, 411.
- (48) Fita, P.; Punzi, A.; Vauthey, E. Local viscosity of binary water +glycerol mixtures at liquid/liquid interfaces probed by time-resolved surface second harmonic generation. *J. Phys. Chem. C* **2009**, *113*, 20705.
- (49) Punzi, A.; Martin-Gassin, G.; Grilj, J.; Vauthey, E. Effect of salt on the excited-state dynamics of malachite green in bulk aqueous solutions and at air/water interfaces: a femtosecond transient absorption and surface second harmonic generation study. *J. Phys. Chem. C* **2009**, *113*, 11822.
- (50) Martin-Gassin, G.; Villamaina, D.; Vauthey, E. Nonradiative deactivation of excited hemicyanines studied with submolecular spatial resolution by time-resolved surface second harmonic generation at liquid-liquid interfaces. *J. Am. Chem. Soc.* **2011**, *133*, 2358.
- (51) Ephardt, H.; Fromhertz, P. Fluorescence and photoisomerization of an amphiphilic aminostibazolum dye as controlled by the sensitivity of radiationless deactivation to polarity and viscosity. *J. Phys. Chem.* **1989**, *93*, 7717.
- (52) Cao, X.; Tolbert, R. W.; McHale, J. L.; Edwards, W. D. Theoretical study of solvent effects on the intramolecular charge transfer of a hemicyanine dye. *J. Phys. Chem. A* **1998**, *102*, 2739.
- (53) Kunz, W.; Lo Nostro, P.; Ninham, B. W. The present state of affairs with Hofmeister effects. *Curr. Opin. Colloid Interface Sci.* **2004**, *9*, 1.
- (54) Ball, P. Water as an active constituent in cell biology. *Chem. Rev.* **2007**, *108*, 74.

- (55) Zhang, Y.; Cremer, P. S. Interactions between macromolecules and ions: the Hofmeister series. *Curr. Opin. Chem. Biol.* **2006**, *10*, 658.
- (56) Jungwirth, P.; Tobias, D. J. Specific ion effects at the air/water interface. *Chem. Rev.* **2006**, *106*, 1259.
- (57) Petersen, P. B.; Saykally, R. J. Probing the interfacial structure of aqueous electrolytes with femtosecond second harmonic generation spectroscopy. *J. Phys. Chem. B* **2006**, *110*, 14060.
- (58) Fedoseeva, M.; Fita, P.; Punzi, A.; Vauthey, E. Salt effect on the formation of dye aggregates at liquid/liquid interfaces studied by time-resolved surface second harmonic generation. *J. Phys. Chem. C* **2010**, *114*, 13774.
- (59) Onorato, R. M.; Otten, D. E.; Saykally, R. J. Adsorption of thiocyanate ions to the dodecanol/water interface characterized by UV second harmonic generation. *Proc. Natl. Acad. Sci. U.S.A.* **2009**, *106*, 15176.
- (60) Viswanath, P.; Aroti, A.; Motschmann, H.; Leontidis, E. Vibrational sum frequency generation spectroscopic investigation of the interaction of thiocyanate ions with zwitterionic phospholipid monolayers at the air/water interface. *J. Phys. Chem. B* **2009**, *113*, 14816.
- (61) Parsons, D. F.; Bostrom, M.; Nostro, P. L.; Ninham, B. W. Hofmeister effects: interplay of hydration, nonelectrostatic potentials, and ion size. *Phys. Chem. Chem. Phys.* **2011**, *13*, 12352.
- (62) Wernersson, E.; Heyda, J.; Vazdar, M.; Lund, M.; Mason, P. E.; Jungwirth, P. Orientational dependence of the affinity of guanidinium ions to the water surface. *J. Phys. Chem. B* **2011**, *115*, 12521.
- (63) Xu, M.; Tang, C. Y.; Jubb, A. M.; Chen, X.; Allen, H. C. Nitrate anions and ion pairing at the air-aqueous interface. *J. Phys. Chem. C* **2009**, *113*, 2082.
- (64) Shamay, E. S.; Richmond, G. L. Ionic disruption of the liquid-liquid interface. *J. Phys. Chem. C* **2010**, *114*, 12590.
- (65) Antoine, R.; Tamburello-Luca, A. A.; Hébert, P.; Brevet, P. F.; Girault, H. H. Picosecond dynamics of eosin B at the air/water interface by time-resolved second harmonic generation: orientational randomization and rotational relaxation. *Chem. Phys. Lett.* **1998**, *288*, 138.
- (66) Fita, P.; Fedoseeva, M.; Vauthey, E. Ultrafast excited-state dynamics of eosin B: a potential probe of the hydrogen-bonding properties of the environment. *J. Phys. Chem. A* **2011**, *115*, 2465.
- (67) Fürstenberg, A.; Vauthey, E. Excited state dynamics of the fluorescent probe lucifer yellow in liquid solutions in heterogeneous media. *Photochem. Photobiol. Sci.* **2005**, *260*.
- (68) Sherin, P. S.; Grilj, J.; Tsentalovitch, Y. P.; Vauthey, E. Ultrafast excited-state dynamics of kynurenine, a UV filter of the human eye. *J. Phys. Chem. B* **2009**, *113*, 4953.
- (69) Fita, P.; Fedoseeva, M.; Vauthey, E. Hydrogen-bond-assisted excited-state deactivation at liquid/water interfaces. *Langmuir* **2011**, *27*, 4645.
- (70) Valdes-Aguilera, O.; Neckers, D. C. Aggregation phenomena in xanthene dyes. *Acc. Chem. Res.* **1989**, *22*, 171.
- (71) Barbara, P. F.; Meyer, T. J.; Ratner, M. A. Contemporary issues in electron transfer research. *J. Phys. Chem.* **1996**, *100*, 13148.
- (72) Vauthey, E. Investigations of bimolecular photoinduced electron transfer reactions in polar solvents using ultrafast spectroscopy. *J. Photochem. Photobiol. A* **2006**, *179*, 1.
- (73) McArthur, E. A.; Eisenthal, K. B. Ultrafast excited-state electron transfer at an organic liquid/aqueous interface. *J. Am. Chem. Soc.* **2006**, *128*, 1068.
- (74) Benjamin, I. Static and dynamic electronic spectroscopy at liquid interfaces. *Chem. Rev.* **2006**, *106*, 1212.
- (75) Nelson, K. V.; Benjamin, I. Electronic absorption line shapes at the water liquid/vapor interface. *J. Phys. Chem. B* **2012**, *116*, 4286.